Infrared spectroscopic identification of the methylsilylidyne (SiCH$_3$, X^{2}A″) and the silenyl (H$_2$CSiH, X^{2}A′) radicals in methane–silane matrices

Chris J. Bennett [a], David Sillars [a], Yoshihiro Osamura [b], Ralf I. Kaiser [a,*]

[a] *Department of Chemistry, University of Hawai'i at Manoa, 2545 The Mall (Bil 301A), Honolulu, HI 96822, USA*
[b] *Department of Chemistry, Rikkyo University, 3-34-1 Nishi-ikebukuro, Tokyo 171-8501, Japan*

Received 1 January 2005; in final form 12 January 2005

Abstract

The methylsilylidyne (SiCH$_3$, X^{2}A″) and the silenyl (H$_2$CSiH, X^{2}A′) radicals were identified via infrared spectroscopy in low temperature silane–methane matrices upon irradiation of the samples matrices with energetic electrons at 10 K. The v_4 and v_3 fundamentals of the methylsilylidyne species were detected at 1226 and 1371 cm^{-1}, whereas one band of the silenyl radical showed up at 822 cm^{-1}(v_6). These assignments were verified in partially deuterated matrices. Our studies suggest that these radicals are generated through radiolysis of silene (H$_2$CSiH$_2$, X^{1}A$_1$) and its methylsilylene isomer (CH$_3$SiH, X^{1}A′). The new absorptions of two SiCH$_3$ isomers can be utilized in future spectroscopic studies of chemical vapor deposition processes and in astronomical searches of silicon-bearing organometallic molecules to better understand the chemistry of the circumstellar envelope of the carbon star IRC + 10216.

1. Introduction

Untangling the formation of silicon-bearing molecules in extraterrestrial environments is an important means to understand the astrochemical evolution of circumstellar envelopes of, for instance, dying carbons stars like IRC + 10216 [1]. So far, seven silicon containing molecules have been detected in their circumstellar shells. These are: silicon carbide (SiC), silicon nitride (SiN), silicon cyanide (SiCN), and tetracarbonsilicide (CCCCSi) together with two cyclic molecules (SiC$_2$, SiC$_3$) [2,3]. Here, the silane and the methane molecules – potential precursors to form complex organo silicon molecules – have also been detected in the outflow of IRC + 10216 via infrared telescopes. Since chemistry in

the inner regions of the circumstellar shells is triggered by photochemistry and by bimolecular as well as termolecular reactions of the photo fragments like the methyl and silyl radicals (CH$_3$(X^{2}A$_2$) and SiH$_3$(X^{2}A$_1$)), carbene and silylene (CH$_2$(X^{3}B$_1$) and SiH$_2$(X^{3}B$_1$)), as well as methylidyne and silylidyne (CH(X$^2\Pi_\Omega$) and SiH(X$^2\Pi_\Omega$)) species, a rich, silicon-based organometallic chemistry is expected to occur.

Small organosilane molecules and radicals of the formula SiCH$_x$ ($x = 1 - 6$) are also important precursors to synthesize amorphous silicon carbide (*a*: Si–C) films via chemical vapor deposition (CVD) on the industrial scale [4,5]. Silicon carbide (SiC) presents a promising class of materials for high temperature and high power electronic devices [6–9]. Actual reaction networks which model the CVD processes of organo silanes [10,11] demand crucial input parameters like rate constants of the critical reactions involved, the reaction intermediates together with the final reaction products, and their

thermochemical data [12–18]. Here, a comprehensive knowledge of the infrared absorption features helps to monitor chemical evolution of CVD processes in real time not only via mass spectrometry [7], but also through time resolved infrared spectroscopy. Combining the models and the spectroscopic investigations of CVD processes will ultimately contribute to optimize the growth processes of amorphous silicon carbide films.

Very recently, we launched a research program to investigate experimentally and computationally the vibrational levels of unstable organo-silicon molecules in low temperature matrices. So far, we have identified six Si_2H_x species disilane ($Si_2H_6(X\,^1A_{1g})$), the *disilyl* radical ($Si_2H_5(X\,^2A')$) [19], two Si_2H_4 isomers silylsilylene ($H_3SiSiH(X\,^1A')$) and disilene ($H_2SiSiH_2(X\,^1A_g)$), as well as the *disilenyl* species ($Si_2H_3(X\,^2A)$) in low temperature silane matrixes [20]. Likewise, we have probed three $SiCH_x$ molecules, namely methylsilane ($SiCH_6(X\,^1A_1)$) together with two $SiCH_5$ isomers *methylsilyl* (CH_3SiH_2- ($X\,^2A'$)) and *silylmethyl* ($SiH_3CH_2(X\,^2A')$), in methane–silane matrices; the vibrational levels of those species in italics were detected for the first time. However, although the infrared spectroscopic properties of the $SiCH_4$ species silene ($H_2CSiH_2(X\,^1A_1)$) and its methylsilylene isomer ($CH_3SiH(X\,^2A')$) are well known [21,22], the vibrational levels of the simpler methylsilylidyne ($SiCH_3(X\,^2A'')$) and silenyl ($H_2CSiH(X\,^2A')$) radicals have been only assigned tentatively via negative ion photoelectron spectroscopy to be 610 ± 15 cm^{-1} as well as 490 ± 10 and 830 ± 10 cm^{-1}, respectively [23]. In this Letter, we present the first direct, infrared spectroscopic identification of these species together with their partially deuterated counterparts in low temperature silane–methane matrices. A complete description of the $SiCH_3$ and $SiCH_4$ potential energy surfaces is given in a forthcoming publication.

2. Experimental

The experiments were carried out in an ultrahigh vacuum (UHV) chamber. Briefly, the vessel consists of a cylindrical stainless steel chamber which can be pumped down to 8×10^{-11} Torr by a magnetically suspended turbopump backed by an oil-free scroll pump. A closed cycle helium refrigerator is interfaced to the machine and holds a polished silver crystal. Cooled to 11.0 ± 0.5 K, the latter serves as a substrate for the ice condensate. The silane–methane ices of thicknesses of 195 ± 25 nm and composition of $1.3 \pm 0.1:1$ were prepared at 11 K by depositing silane (99.99%) and methane (99.99%) at pressures of 8×10^{-8} Torr for 20 min onto the cooled silver crystal (Table 1); the infrared absorptions of the frosts are summarized in Table 1 [24]. These ices were irradiated with 5 keV electrons generated in an electron gun at beam currents of 1000 nA

Table 1
Infrared absorptions of the methane–silane frosts (sh: shoulder); α, β, and γ denote lattice modes of the methane–silane sample

Frequency, cm^{-1}	Assignment	Carrier molecule
4523	$v_2 + v_3$	CH_4
4364	$2v_3$	SiH_4
4358	$v_3 + v_4$	CH_4
4298	$v_3 + v_4$	CH_4
4292	$v_1 + v_3$	SiH_4
4200	$v_1 + v_4$	CH_4
4112	$v_2 + 2v_4$	CH_4
3852/3895	$3v_4$	CH_4
–	$v_3 + v_4 + \beta$	SiH_4
3139	$v_2 + v_3$	SiH_4
–	$v_3 + v_4 + \alpha$	SiH_4
3074	$v_3 + v_4$	SiH_4
3011	v_3	CH_4
2815	$v_2 + v_4$	CH_4
2595	$2v_4$	CH_4
2306	$v_3 + \gamma$	SiH_4
–	$v_3 + \beta$	SiH_4
2193	$v_3 + \alpha$	SiH_4
2164	v_3	SiH_4
1878	$v_2 + v_4 + \alpha$	SiH_4
1300	v_4	CH_4
1032	$v_2 + \beta/v_4 + \gamma$	SiH_4
1032	$v_2 + \beta/v_4 + \gamma$	SiH_4
961	v_2	SiH_4
930	$v_4 + \beta$	SiH_4
914	$v_4 + \alpha$	SiH_4
883	v_4	SiH_4

for up to 3 h by scanning the electron beam for 3 h over the target area of 3.0 ± 0.4 cm^2. The reaction products were detected on line and in situ via a Fourier transform infrared spectrometer (Nicolet 510 DX; 5000–500 cm^{-1}) operating in an absorption–reflection–absorption mode (reflection angle $\alpha = 75°$) (resolution 4 cm^{-1}). The line shapes in the matrix have been fitted successfully with Gaussian profiles – an approach which yielded better results than Lorentzian peak profiles. Within the signal to noise level, this procedure yielded excellent fits despite potential site heterogeneities in the matrix.

3. Theoretical approach

We have employed the hybrid density functional B3LYP method [25] with the 6-311G(d,p) basis functions in order to obtain the optimized structures and vibrational frequencies for $SiCH_x$ ($x = 4, 3, 2, 1$) systems. The relative energies are calculated by using the coupled cluster CCSD(T) method [26,27] with the aug-cc-pVTZ basis functions [28] at the structures obtained by the B3LYP method with the correction of B3LYP zero-point vibrational energies without scaling. All calculations were carried out with GAUSSIAN 98 program package [29]. To analyze the infrared spectra for the species obtained by present experiments, we have also

calculated the vibrational frequencies and infrared intensities for various SiCH$_x$ ($x = 4, 3, 2, 1$) isomers and for the partially deuterated species as compiled in Table 2; the structures of various SiCH$_4$, SiCH$_3$, SiCH$_2$, and SiCH isomers are shown in Fig. 1.

4. Results

The infrared data propose that the response of the silane–methane matrix upon the electron bombardment is directed by an early synthesis of the silyl, SiH$_3$(X^{2}A$_1$),

Table 2
Unscaled vibrational frequencies (cm^{-1}) and their infrared intensities (km mol^{-1}) of various SiCH$_4$, SiCH$_3$, SiCH$_2$, and SiCH isomers together with their partially deuterated counterparts calculated with B3LYP/6-311G(d,p) method

		Frequencies	Intensities, km mol^{-1}	Frequencies	Intensities, km mol^{-1}	Characterization
SiCH$_4$						
		(4) H$_2$C=SiH$_2$ (^{1}A$_1$)		H$_2$C=SiD$_2$		
ν_1	a$_1$	3143	0	3143	0	CH$_2$ sym. str.
ν_2	a$_1$	2265	31	1623	20	SiH$_2$ sym. str.
ν_3	a$_1$	1401	9	1399	6	CH$_2$ scissor
ν_4	a$_1$	997	23	983	5	C–Si str.
ν_5	a$_1$	943	28	684	23	SiH$_2$ scissor
ν_6	a$_2$	730	0	662	0	Twist
ν_7	b$_1$	782	52	764	64	CH$_2$ out-of-plane
ν_8	b$_1$	455	30	353	16	SiH$_2$ out-of-plane
ν_9	b$_2$	3231	0	3231	0	CH$_2$ asym. str.
ν_{10}	b$_2$	2288	94	1656	57	SiH$_2$ asym. str.
ν_{11}	b$_2$	841	80	788	56	CH$_2$ rocking
ν_{12}	b$_2$	485	6	395	8	SiH$_2$ rocking
		(5) H$_3$C–SiH (^{1}A′)		H$_3$C–SiD		
ν_1	a′	3104	15	3104	14	CH$_3$ asym. str.
ν_2	a′	2993	4	2993	4	CH$_3$ sym. str.
ν_3	a′	2005	320	1443	170	SiH str.
ν_4	a′	1437	6	1437	5	CH$_3$ deformation
ν_5	a′	1267	23	1266	23	CH$_3$ umbrella
ν_6	a′	952	82	860	38	SiH bend, CH$_3$ rock
ν_7	a′	662	53	648	60	C–Si str.
ν_8	a′	629	10	523	10	SiH bend
ν_9	a″	3045	15	3045	15	CH$_3$ asym. str.
ν_{10}	a″	1453	13	1453	13	CH$_3$ deformation
ν_{11}	a″	578	3	564	3	CH$_3$ rocking
ν_{12}	a″	150	0	129	0	Torsion
		(5′) H$_3$C–SiH (^{3}A″)		H$_3$C–SiD		
ν_1	a′	3112	5	3112	5	CH$_3$ asym. str.
ν_2	a′	3023	9	3022	9	CH$_3$ sym. str.
ν_3	a′	2160	91	1555	43	SiH str.
ν_4	a′	1453	10	1452	11	CH$_3$ deformation
ν_5	a′	1269	0	1268	0	CH$_3$ umbrella
ν_6	a′	883	71	837	49	CH$_3$ rocking
ν_7	a′	659	11	657	11	C–Si str.
ν_8	a′	557	7	435	7	SiH bend
ν_9	a″	3096	3	3096	3	CH$_3$ asym. str.
ν_{10}	a″	1456	8	1456	8	CH$_3$ deformation
ν_{11}	a″	794	17	793	17	CH$_3$ rocking
ν_{12}	a″	124	0	102	0	Torsion
		(6) HC–SiH$_3$ (^{3}A″)		HC–SiD$_3$		
ν_1	a′	3264	1	3263	1	CH str.
ν_2	a′	2222	82	1569	33	SiH$_3$ sym. str.
ν_3	a′	2198	80	1600	67	SiH$_3$ asym. str.
ν_4	a′	953	218	687	74	CH$_3$ umbrella
ν_5	a′	943	55	677	33	SiH$_3$ deformation
ν_6	a′	800	25	806	77	C–Si str.
ν_7	a′	641	50	492	33	SiH$_3$ rocking
ν_8	a′	326	30	322	26	CH bend
ν_9	a″	2195	120	1585	72	SiH$_3$ asym. str.
ν_{10}	a″	946	52	679	30	SiH$_3$ deformation
ν_{11}	a″	633	48	483	29	SiH$_3$ deformation
ν_{12}	a″	116	35	115	35	Torsion

Table 2 (continued)

		Frequencies	Intensities, km mol^{-1}	Frequencies	Intensities, km mol^{-1}	Characterization
SiCH$_3$						
		(7) H$_3$C–Si (^{2}A″)		D$_3$C–Si		
ν_1	a′	3040	20	2236	9	CH$_3$ asym. str.
ν_2	a′	2965	4	2133	1	CH$_3$ sym. str.
ν_3	a′	1445	22	1051	8	CH$_3$ deformation
ν_4	a′	1259	22	977	33	CH$_3$ umbrella
ν_5	a′	665	54	606	42	C–Si str.
ν_6	a′	528	4	406	3	CH$_3$ rocking
ν_7	a″	3072	7	2272	3	CH$_3$ asym. str.
ν_8	a″	1359	14	976	8	CH$_3$ deformation
ν_9	a″	598	8	456	4	CH$_3$ deformation
		(8) H$_2$C=SiH (^{2}A′)		H$_2$C=SiD		
ν_1	a′	3223	0	3223	0	CH$_2$ asym. str.
ν_2	a′	3116	0	3116	0	CH$_2$ sym. str.
ν_3	a′	2128	66	1534	37	SiH str.
ν_4	a′	1368	5	1368	4	CH$_2$ scissor
ν_5	a′	964	4	961	3	C–Si str.
ν_6	a′	839	64	759	44	SiH bend, CH$_2$ rock
ν_7	a′	521	1	429	4	SiH bend, CH$_2$ rock
ν_8	a″	749	56	727	56	out-of-plane
ν_9	a″	256	4	231	3	Torsion
		(10) HC=SiH$_2$ (^{2}B$_2$)		HC=SiD$_2$		
ν_1	a$_1$	3343	15	3343	15	CH str.
ν_2	a$_1$	2254	21	1612	13	SiH$_2$ sym. str.
ν_3	a$_1$	1072	6	1067	4	C–Si str.
ν_4	a$_1$	958	45	689	24	SiH$_2$ scissor
ν_5	b$_1$	667	17	614	30	out-of-plane
ν_6	b$_1$	319	44	263	28	out-of-plane
ν_7	b$_2$	2265	88	1641	54	SiH$_2$ asym. str.
ν_8	b$_2$	606	44	465	29	SiH$_2$ rocking
ν_9	b$_2$	196	43	195	42	CH bend
		(9) C–SiH$_3$ (^{2}A″)		C–SiD$_3$		
ν_1	a′	2209	64	1586	46	SiH$_3$ asym. str.
ν_2	a′	2154	28	1541	19	SiH$_3$ sym. str.
ν_3	a′	958	80	675	20	SiH$_3$ deformation
ν_4	a′	872	96	598	70	SiH$_3$ umbrella
ν_5	a′	681	29	728	21	C–Si str.
ν_6	a′	261	42	200	28	SiH$_3$ rocking
ν_7	a″	2215	105	1602	64	SiH$_3$ asym. str.
ν_8	a″	883	45	634	26	SiH$_3$ deformation
ν_9	a″	456	37	346	24	SiH$_3$ deformation
Singlet SiCH$_2$						
		(11) H$_2$C=Si (^{1}A$_1$)		D$_2$C=Si		
ν_1	a$_1$	3083	0	2242	1	CH$_2$ sym. str.
ν_2	a$_1$	1350	28	1090	33	CH$_2$ scissor
ν_3	a$_1$	951	13	830	2	C–Si str.
ν_4	b$_1$	722	133	569	83	out-of-plane
ν_5	b$_2$	3153	1	2336	1	CH$_2$ asym. str.
ν_6	b$_2$	362	0	277	0	CH$_2$ rocking
		(12) trans-bent HC=SiH (^{1}A′)		HC=SiD		
ν_1	a′	3288	3	3288	3	CH str.
ν_2	a′	2227	19	1608	9	SiH str.
ν_3	a′	1107	11	1095	14	SiC str.
ν_4	a′	785	78	778	84	CH bend
ν_5	a′	347	72	264	41	SiH bend
ν_6	a″	603	102	586	96	Torsion
		(13) C=SiH$_2$ (^{1}A$_1$)		C=SiD$_2$		
ν_1	a$_1$	2224	11	1590	5	SiH sym. str.
ν_2	a$_1$	951	0	920	7	C–Si str.
ν_3	a$_1$	811	53	601	27	SiH$_2$ scissor

Table 2 (*continued*)

		Frequencies	Intensities, km mol^{-1}	Frequencies	Intensities, km mol^{-1}	Characterization
v_4	b_1	359	0	273	0	out-of-plane
v_5	b_2	2264	44	1640	29	SiH$_2$ asym. str.
v_6	b_2	267	66	205	49	SiH$_2$ rocking
	Linear HCSi ($^2\Sigma_g$)			DCSi		
v_1	σ_g	3270	2	2427	4	CH str.
v_2	σ_g	1049	25	1012	23	C–Si str.
v_3	π	574	135	444	80	Bend
v_4	π'	505	14	390	8	Bend

and methyl, CH$_3$(X^{2}A$_2$), radicals plus atomic hydrogen. The v_2 modes of the silyl and methyl radicals are visible at 723 and 609 cm^{-1}, respectively. These data agree well with previous matrix studies [30–32]. Very strong absorptions of ethane (C$_2$H$_6$(X^{1}A$_{1g}$) (2973 cm^{-1}, v_{10}; 2881 cm^{-1}, v_5; 1464 cm^{-1}, v_{11}; 1381 cm^{-1}, v_{16}; 827 cm^{-1}, v_{12}) and silane (Si$_2$H$_6$(X^{1}A$_{1g}$)) (2142 cm^{-1}, $v_{4/5}$; 936 cm^{-1}, v_{11}; 825 cm^{-1}, v_6) showed up, too. As the irradiation time increased, the matrix behaved similarly to the pure methane and silane systems [19,20]. First, we were able to observe the electron-induced radiolysis sequence from ethane via the ethyl radical (C$_2$H$_5$(X^{2}A$'$)), ethylene (C$_2$H$_4$(X^{1}A$_g$)), and the vinyl radical (C$_2$H$_3$(X^{2}A$'$)) to form finally acetylene (C$_2$H$_2$(X$^1\Sigma_g^+$)). This has been documented via absorptions observed at 2939 cm^{-1} (v_2), 2848 cm^{-1} (v_3), and 531 cm^{-1} (v_2) (ethyl radical), 1440 cm^{-1} (v_{12}), 960 cm^{-1} (v_7), and 826 cm^{-1} (v_{12}) (ethylene), 897 cm^{-1} (v_8) and 688 cm^{-1} (v_7) (vinyl radical) and ultimately at 3282 cm^{-1} (v_3) and 736 cm^{-1} (v_5) (acetylene). Secondly, a similar reaction sequence was verified for the fragmentation of the disilane molecule, i.e., observing the 852 cm^{-1} (v_6) band of the disilyl radical (Si$_2$H$_5$(X^{2}A$'$)), the two Si$_2$H$_4$ isomers silylsilylene (H$_3$SiSiH(X^{1}A$'$); 856 cm^{-1} (v_5)) and disilene (H$_2$Si-SiH$_2$(X^{1}A$_g$); 897 cm^{-1} (v_{11})), disilenyl (H$_2$SiSiH(X^{2}A); 933 cm^{-1} (v_4)), and the bridged disilicondihydride (SiH$_2$-Si(X^{1}A$_1$); 1098 cm^{-1} (v_6)).

Having attributed the absorptions which also appear in the pure methane and silane ices upon radiation exposure, we investigate now additional, hitherto unassigned features in the infrared spectra of the irradiated silane–methane matrix. At low radiation doses, six prominent absorptions of the methyl silane molecule, CH$_3$SiH$_3$ (X^{1}A$_1$), appear at 2143 cm^{-1} (v_2), 1254 cm^{-1} (v_3), 976 cm^{-1} (v_4), 946 cm^{-1} (v_{10}), 863 cm^{-1} (v_{11}), and 691 cm^{-1} (v_5) (Table 3). Also, we were able to identify two SiCH$_5$ isomers. These are methylsilyl, CH$_3$SiH$_2$(X^{2}A$'$), and silylmethyl, SiH$_3$CH$_2$(X^{2}A$'$), via their absorptions at 1251 cm^{-1} (v_5), 1414 cm^{-1} (v_{12}), and 653 cm^{-1} (v_8), as well as 645 cm^{-1} (v_8), respectively. These findings are in excellent agreement with a previous, low current (78.8 nA) electron exposure of silane–methane matrices [24].

The identification of the methylsilyl and silylmethyl radicals invites to investigate how the methane–silane

ices responds to an enhanced irradiation time. As the electron exposure increases, novel absorptions appear at 742 and 1947 cm^{-1}. These absorptions could not be assigned to any of the molecules discussed in the previous paragraphs. Instead, a comparison with our computed vibration frequencies of the SiCH$_4$ isomers (Fig. 1 and Table 2) suggest – after scaling by a factor of 0.97 – an assignment of to the thermodynamically more stable silene molecule (H$_2$CSiH$_2$, X^{1}A$_1$) (740 cm^{-1}; v_7, second strongest absorption) and to the less favorable methylsilylene isomer (CH$_3$SiH, X^{1}A$'$) (v_3, 1947 cm^{-1}); this presents an excellent agreement with the calculations and also with previous experimental studies [33,34]. Note that the most intense v_{10} fundamental of silene could not be observed since it overlaps with those features appearing in the silane–methane matrix; likewise the v_2, v_4, and v_5 modes coincide with absorptions from the matrix material, from the methyl silane molecule, and from the silane species. On the other hand, the v_3 peak of the methylsilylene species has the strongest absorption coefficient of all fundamentals. The second strongest mode of this isomer (v_6) is obscured by the disilane molecule, too. We can also utilize the absorption coefficients to quantify the ratios of the silene and of the methylsilylene isomers to be 30 ± 10:1; this suggest a preferential formation of the thermodynamically – by 10 kJ mol^{-1} – more stable silene isomer. Note that, we were unable to identify the least stable SiCH$_4$ isomer, the silylmethylene species (HCSiH$_3$, X^{3}A$''$); the latter is less favorable by 197 kJ mol^{-1} compared to the silene molecule. The formation of both the silene and the methylsilylene molecules has been also been verified in d4–silane–methane matrices. Here, we detected the d2–silene molecule (H$_2$CSiD$_2$, X^{1}A$_1$) at 711 cm^{-1} (v_5) and 952 cm^{-1} (v_8). The peak positions agree well with a previous study by Margrave et al. [33]. Likewise, the d1-methylsilylyne isomer, CH$_3$SiD, X^{1}A$'$, was verified via its absorptions at 1402 cm^{-1} (v_3), 833 cm^{-1} (v_6), and 641 cm^{-1} (v_3, shoulder) (Table 3).

As the irradiation time rises even further, we attempted to synthesize various SiCH$_3$ isomers (Figs. 1 and 2) via an atomic hydrogen elimination from both SiCH$_4$ isomers. Of the four lowest lying isomers investigated computationally, i.e., H$_3$CSi(X^{2}A$''$) (0 kJ mol^{-1}), H$_2$C=SiH(X^{2}A$'$) (+53 kJ mol^{-1}), HC=SiH$_2$(X^{2}B$_2$)
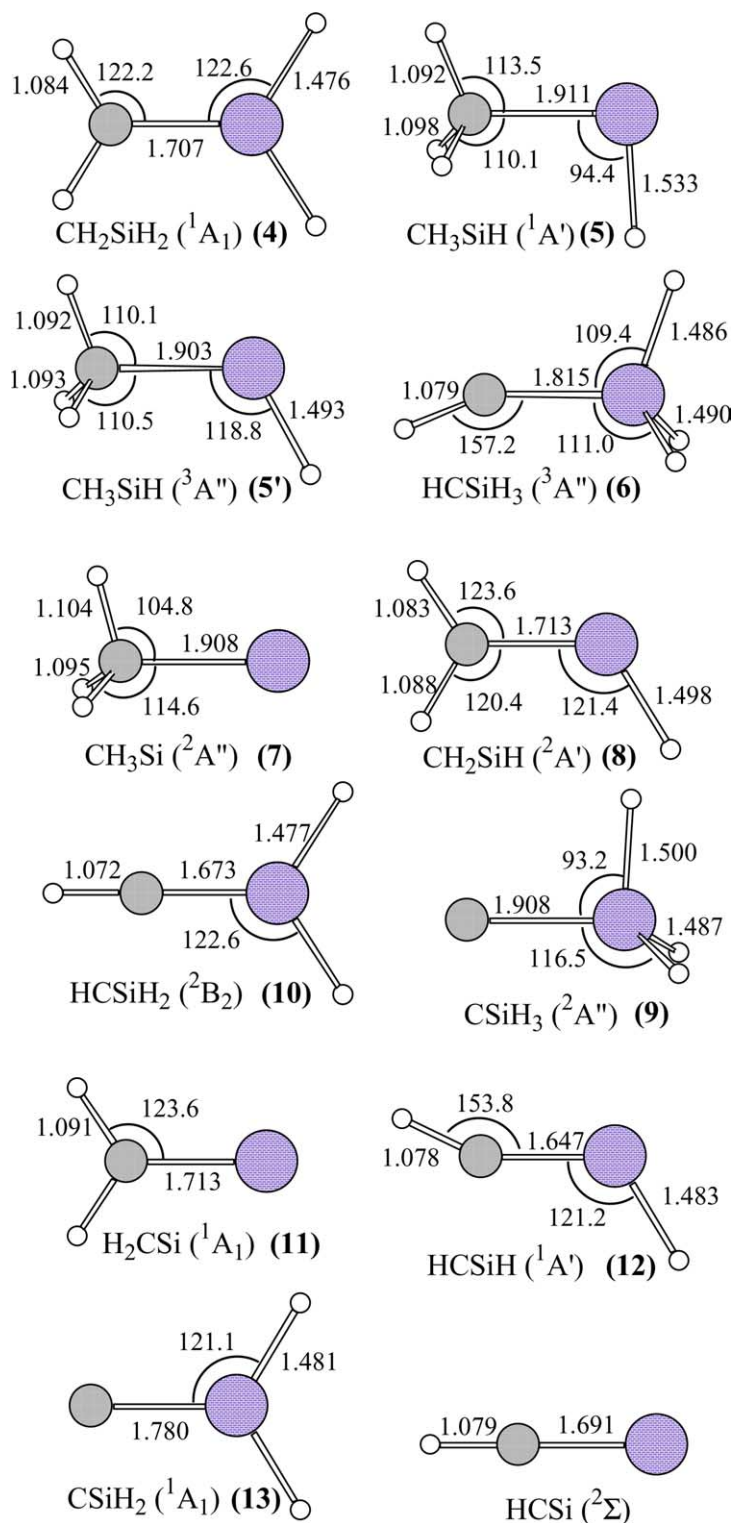
Fig. 1. Optimized structures of SiCH$_4$, SiCH$_3$, SiCH$_2$, and SiCH species calculated with the B3LYP/6-311 G(d,p) method. The bond lengths and bond angles are given in units of Å and degrees, respectively.

(+128 kJ mol^{-1}), and CSiH$_3$(X^{2}A″) (+337 kJ mol^{-1}), only the two energetically most stable species were positively identified for the first time via infrared spectroscopy; the relative energies are given in parenthesis.

Here, absorptions at 1226 cm^{-1} (v_4) and 1371 cm^{-1} (v_3) were assigned to the H$_3$CSi(X^{2}A″) structure; the peak at 822 cm^{-1} (v_6) could be attributed to the less stable – by 53 kJ mol^{-1} – H$_2$C=SiH(X^{2}A′) isomer (Fig. 2,

Table 3
Compilation of observed $SiCH_x$ (x = 6–2) species in low temperature methane–silane matrices; both the H_3CSi and the H_2CSiH isomers have been detected for the first time via infrared spectroscopy

Frequency, cm^{-1}	Fundamental	Carrier
691	v_5	CH_3SiH_3
863	v_{11}	CH_3SiH_3
946	v_{10}	CH_3SiH_3
976	v_4	CH_3SiH_3
1254	v_3	CH_3SiH_3
2143	v_2	CH_3SiH_3
653	v_8	CH_3SiH_2
1414	v_{12}	CH_3SiH_2
1251	v_5	CH_3SiH_2
645	v_8	CH_2SiH_3
740	v_7	H_2CSiH_2
1947	v_3	CH_3SiH
1211	v_4	H_3CSi
1387	v_3	H_3CSi
717	v_8	H_2CSiH
688	v_4	H_2CSi

Table 3). These data are in excellent agreement with our calculated values – scaled by 0.97–0.95. Our finding also support Bengali et al.'s photoelectron spectroscopy experiment. Here, Bengali et al. determined the positions of the v_5 band of the methylsilylidyne species to be 610 ± 15 cm^{-1}; likewise, two absorptions at 490 ± 10 and 830 ± 10 cm^{-1} were assigned as the v_7 and v_6 fundamentals. Note that due to the limits of our detector system, we were unable to confirm the position of the v_7 mode. However, our experiments verified the assignment of the v_6 fundamental to be 820 cm^{-1}. Note that as the irradiation time is raised even further, we noticed pronounced absorptions at 688 cm^{-1} which do not shift in d4–silane–methane ices. These could be assigned to the well known $H_2CSi(X^1A_1)$ structure [35].

Also, we were able to confirm the assignments of the methylsilylidyne and the silenyl species in d4–silane–methane matrix (Fig. 3). Here, the positions of the $H_3CSi(X^2A'')$ peaks shift only by 2 cm^{-1}; peak positions similar to the methane–silane matrix are expected because in the d4–silane–methane matrix, the deuterium is predicted to be bound only to the silicon, but not to the carbon atom. Considering the second isomer, silenyl, we detected absorptions of the d1-species ($H_2C=SiD(X^2A')$ at 701 cm^{-1} (v_8); the 734 cm^{-1} (v_6) feature is obscured by the strong 736 cm^{-1} absorption of acetylene (Fig. 3).

5. Discussion and summary

Our combined theoretical and experimental investigations of irradiated methane–silane and methane–d4–silane matrices verify the synthesis of two $SiCH_3$ isomers: methylsilylidyne ($SiCH_3$, X^2A'') (7) and the silenyl (H_2CSiH, X^2A') radical (8) (Fig. 3). Both species
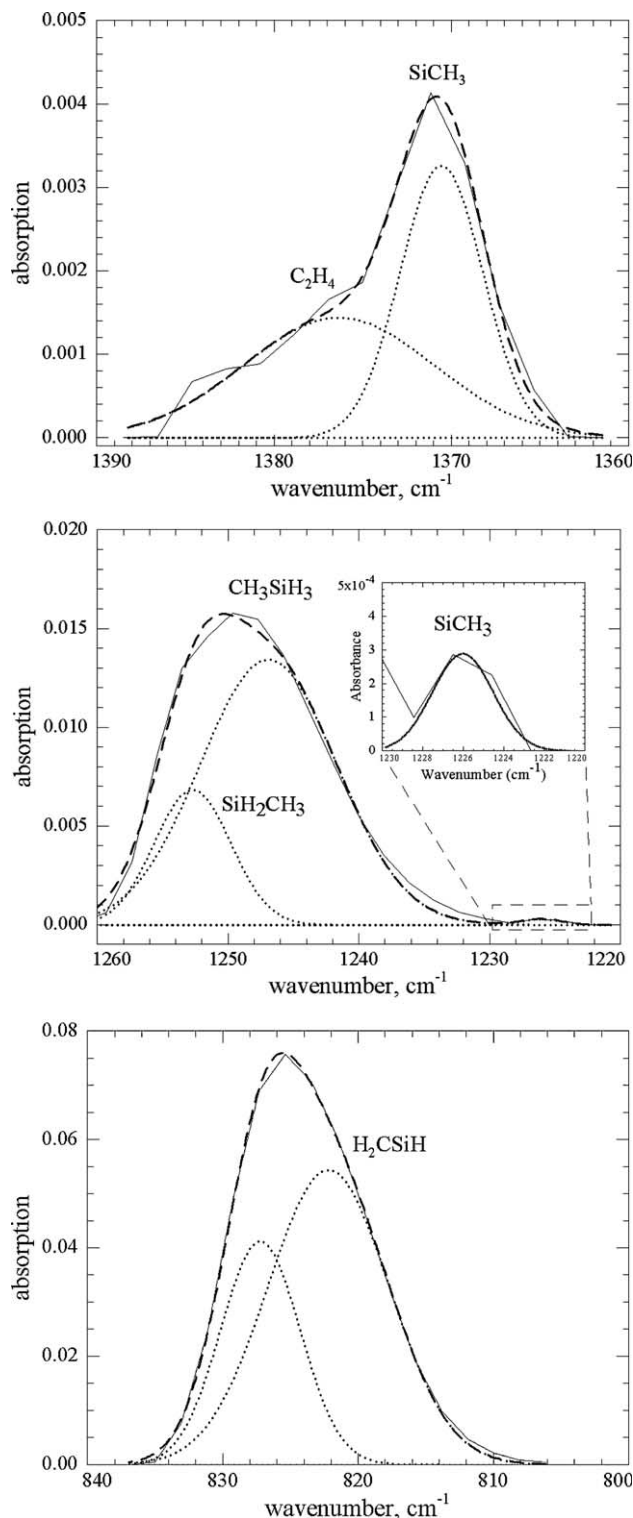

Fig. 2. New absorption features of the methylsilylidyne ($SiCH_3$, X^2A'') and the silenyl (H_2CSiH, X^2A') radicals at 11 K.

were identified through their infrared absorptions (v_4 and v_3) at 1226 and 1371 cm^{-1} (methylsilylidene) as well as 822 cm^{-1} (v_6) (silenyl). The time sequence of the appearance of these fundamentals suggests that both
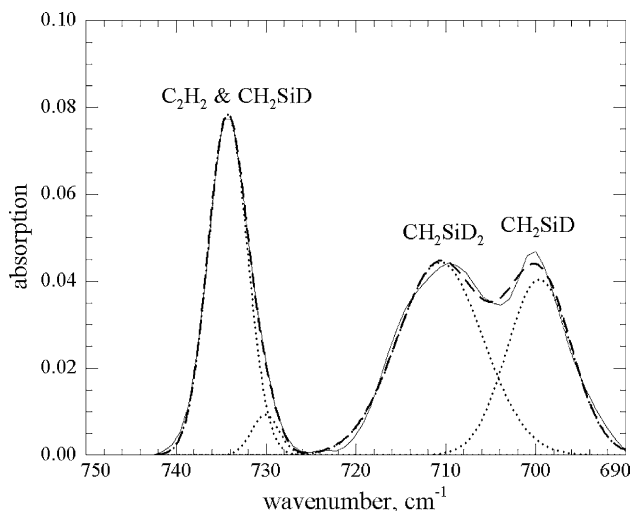
Fig. 3. New absorption feature of the d1–silenyl (H_2CSiD, X^2A') radical in 11 K d4–silane–methane matrices.

radicals are generated through radiolysis of silene (H_2CSiH_2, X^1A_1) (**4**) and its methylsilylene isomer (CH_3SiH, X^1A') (**5**). Both processes are endoergic by 370 kJ mol^{-1} and 360 kJ mol^{-1}, respectively. Note that, we have no evidence on the involvement of a third SiCH$_4$ isomer, i.e., the silylmethylene species (HCSiH$_3$, X^3A'') (**6**). This could be readily understood in terms of the thermochemistry of the reaction since silylmethylene is less stable by 197 kJ mol^{-1} compared to the silene isomer. Also, silylmethylene can only be formed through decomposition of the silylmethyl radical (SiH$_3$CH$_2$(X^2A')) (**3**). However, the later was found to be synthesized at concentrations of a factor of 10 less that the corresponding methylsilyl isomer (CH$_3$SiH$_2$(X^2A')) (**2**). Summarized, the failed detection of silylmethylene species (HCSiH$_3$, X^3A'') (**6**) correlates nicely with the low abundance of the sole silylmethylene precursor, i.e., SiH$_3$CH$_2$(X^2A') (**3**), and also by the unfavorable energetics.

Let us investigate the synthetic routes to methylsilylidyne (SiCH$_3$, X^2A'') (**7**) and the silenyl radical

(H_2CSiH, X^2A') (**8**) in more detail. Methylsilylidyne can only be formed via radiolysis of the methylsilylene isomer (CH$_3$SiH, X^1A') (**5**) (Fig. 4), whereas the silenyl species (H$_2$CSiH, X^2A') (**8**) can be synthesized by degradation of silene (H$_2$CSiH$_2$, X^1A_1) (**4**) and its methylsilylene isomer (CH$_3$SiH, X^1A') (**5**). As the irradiation time increases, we also verified the synthesis of the energetically most stable SiCH$_2$ isomer, i.e., H$_2$CSi(X^1A_1) (**11**) molecule via atomic hydrogen loss from silenyl and methylsilylidyne. As expected from the hydrogen connectivities to the carbon and silicon atoms in the precursor molecules, we would not expect the formation of the H$_2$SiC(X^1A_1) isomer (**13**), simply because neither the silenyl nor the methylsilylidyne molecules has two hydrogen-silicon bonds. Note that H$_2$SiC(X^1A_1) (**13**) is also thermodynamically less stable by 349 kJ mol^{-1} than the H$_2$CSi-(X^1A_1) (**11**) isomer. However, based on the structure of the silenyl radical (H$_2$CSiH, X^2A') (**8**) we would also expect absorptions from the *trans*-HC=SiH(X^1A') isomer (**12**). However, none of the fundamentals was observed in the matrix. Recall that this isomer (**12**) is less stable by 144 kJ mol^{-1} compared to the experimentally observed H$_2$CSi(X^1A_1) molecule (**11**). Therefore, we may conclude that upon energy transfer from the impinging electron to the silenyl radical, the unimolecular decomposition – and the energetics of the reaction – favor the formation of the H$_2$CSi(X^1A_1) isomer (**11**).

Summarized, this Letter completes the infrared spectroscopic detection of a series of hydrogenated silicon–carbon clusters of the generic formula SiCH$_x$ ($x = 6$–1). All low-lying isomers have now been positively identified in low temperature matrices. Their absorptions, and in particular those of the newly detected SiCH$_3$ isomers silenyl and methylsilylidyne can be utilized in future spectroscopic studies of CVD processes and in astronomical searches of silicon-bearing organometallic molecules to better understand the chemistry of the circumstellar envelope of the carbon star IRC + 10216.
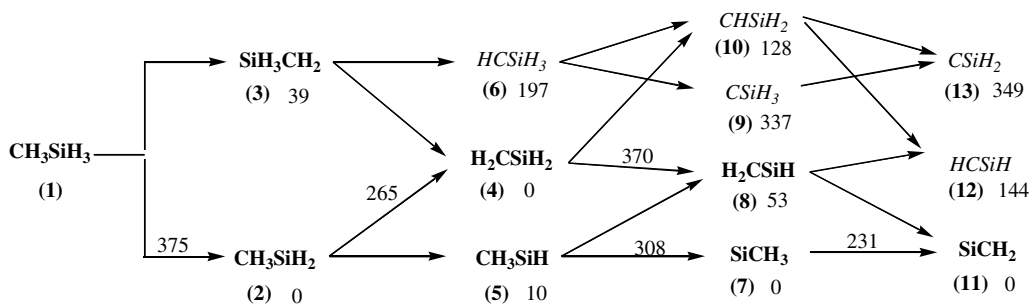

Fig. 4. Electron induced decomposition sequence of methylsilane to form various SiCH$_x$ ($x = 6$–2) isomers in low temperature silane–methane matrices. Species in bold have been detected in our experiments. Relative energies of the isomers and bond dissociation energies calculated with the CCSD(T) method are given in kJ mol^{-1}.

Acknowledgments

References

[1] D.M. Goldhaber, A.L. Betz, Ap. J. 279 (1984) L55.
[2] B.E. Turner, Ap. J. 376 (1991) 573.
[3] R.I. Kaiser, Chem. Rev. 102 (2002) 1309.
[4] K.S. Nahm et al., J. Chem. Eng. Jpn. 34 (2001) 692.
[5] L.V. Interrante, B. Han, J.B. Hudson, C. Whitmarsh, Appl. Surf. Sci. 46 (1990) 5.
[6] M. Shinohara, Y. Kimura, D. Shoji, M. Niwano, Appl. Surf. Sci. 175/176 (2001) 591.
[7] S. Nishino, Y. Hazuki, H. Matsunami, T. Tanaka, J. Electrochem. Soc. 127 (1980) 2674.
[8] K. Shibahara, S. Nishino, H. Matsunami, J. Cryst. Growth 78 (1986) 538.
[9] R. Fantoni, F. Bjnen, N. Djuric, S. Piccirillo, Appl. Phys. B 52 (1991) 176.
[10] S.L. Girshickm, M.T. Swihart, S.M. Hu, M.R. Mahajan, S. Nijhawan, Proc. Electrochem. Soc. 98 (1999) 215.
[11] M.T. Swihart, S.L. Girshick, J. Phys. Chem. B 103 (1999) 64.
[12] P. Ho, M.E. Coltrin, J.S. Binkley, C.F. Melius, J. Phys. Chem. 90 (1986) 3399.
[13] M.C. Ernst, A.F. Sax, J. Kalcher, Chem. Phys. Lett. 216 (1993) 189.
[14] M.T. Swihart, J. Phys. Chem. A. 104 (2000) 6083.
[15] C. Pak, J.C. Rienstra-Kiracofe, H.F. Schaefer, J. Phys. Chem. A 104 (2000) 11232.
[16] S. Hundsicker, R.O. Jones, J. Chem. Phys. 105 (1996) 5048.
[17] M. Pellarin et al., Chem. Phys. Lett. 277 (1997) 96.
[18] Z.Y. Jian et al., Chem. Phys. 290 (2003) 223.
[19] D. Sillars, C.J. Bennett, Y. Osamura, R.I. Kaiser, Chem. Phys. 305 (2004) 143.
[20] D. Sillars, C.J. Bennett, Y. Osamura, R.I. Kaiser, Chem. Phys. Lett. 392 (2004) 541.
[21] V.N. Khabashesku, K.N. Kudin, J.L. Margrave, J. Mol. Struct. 443 (1998) 175.
[22] G. Maier, H.P. Reisenauer, J. Glatthaar, Chem. Eur. J. 8 (2002) 4383.
[23] A.A. Bengali, D.G. Leopold, J. Am. Chem. Soc. 114 (1992) 9192.
[24] D. Sillars, C.J. Bennett, Y. Osamura, R.I. Kaiser, Chem. Phys. (2004) (submitted).
[25] A.D. Becke, J. Chem. Phys. 98 (1993) 5648.
[26] G.D. Purvis, R.J. Bartlett, J. Chem. Phys. 76 (1982) 1910.
[27] K. Raghavachari, G.W. Trucks, J.A. Pople, J.A.M. Head-Gordon, Chem. Phys. Lett. 157 (1989) 479.
[28] T.H. Dunning, J. Chem. Phys. 90 (1989) 1007.
[29] M.J. Frisch et al., Gaussian 98, Revision A.11, Gaussian, Inc., Pittsburgh PA, 2001.
[30] L. Andrews, X. Wang, J. Phys. Chem. A 106 (2002) 7696.
[31] L. Li, J.T. Graham, W. Weltner, J. Phys. Chem. A 105 (2001) 11018.
[32] N. Legay-Sommaire, F. Legay, J. Phys. Chem. A 102 (1998) 8759.
[33] V.N. Khabashesku, K.N. Kudin, J.L. Margrave, J. Mol. Struct. 443 (1998) 175.
[34] G. Maier, H.P. Reisenauer, J. Glatthaar, Chem. Eur. J. 8 (2002) 4383, and references therein.
[35] T.C. Smith, H. Li, D.J. Clouthier, J. Chem. Phys. 114 (2001) 9012.